THE JOURNAL OF BIOLOGICAL CHEMISTRY
Vol. 278, No. 1, Issue of January 3, pp. 357–365, 2003
Printed in U.S.A.


# Snapshots of the Cystine Lyase C-DES during Catalysis

STUDIES IN SOLUTION AND IN THE CRYSTALLINE STATE*

Received for publication, September 25, 2002
Published, JBC Papers in Press, October 16, 2002, DOI 10.1074/jbc.M209862200

**Jens T. Kaiser‡§¶, Stefano Bruno§‖**, Tim Clausen‡, Robert Huber‡, Francesca Schiaretti‖, Andrea Mozzarelli‖‡‡, and Dorothea Kessler§§¶¶**

*From the ‡Max-Planck-Institut für Biochemie, Abt. Strukturforschung, Am Klopferspitz 18a, Martinsried 82152, Germany, the ‖Department of Biochemistry and Molecular Biology and the ‡‡Italian National Institute for the Physics of Matter, University of Parma, Parma 43100, Italy, and the §§Universität Heidelberg, Biochemiezentrum, Heidelberg D-69120, Germany*

**The cystine lyase (C-DES) of *Synechocystis* is a pyridoxal-5′-phosphate-dependent enzyme distantly related to the family of NifS-like proteins. The crystal structure of an N-terminal modified variant has recently been determined. Herein, the reactivity of this enzyme variant was investigated spectroscopically in solution and in the crystalline state to follow the course of the reaction and to determine the catalytic mechanism on a molecular level. Using the stopped-flow technique, the reaction with the preferred substrate cystine was found to follow biphasic kinetics leading to the formation of absorbing species at 338 and 470 nm, attributed to the external aldimine and the α-aminoacrylate; the reaction with cysteine also exhibited biphasic behavior but only the external aldimine accumulated. The same reaction intermediates were formed in crystals as seen by polarized absorption microspectrophotometry, thus indicating that C-DES is catalytically competent in the crystalline state. The three-dimensional structure of the catalytically inactive mutant C-DES$^{K223A}$ in the presence of cystine showed the formation of an external aldimine species, in which two alternate conformations of the substrate were observed. The combined results allow a catalytic mechanism to be proposed involving interactions between cystine and the active site residues Arg-360, Arg-369, and Trp-251*; these residues reorient during the β-elimination reaction, leading to the formation of a hydrophobic pocket that stabilizes the enolimine tautomer of the aminoacrylate and the cysteine persulfide product.**

Iron sulfur (Fe/S) proteins perform important biological functions varying from electron transfer and catalysis to gene regulation and redox sensing (for recent reviews, see Refs. 1 and 2). The Fe/S clusters contained in Fe/S proteins are crucial for these functions and have been characterized in considerable detail by biochemical as well as biophysical methods (1). However, research concerning the biosynthetic assembly of these complexes has intensified only recently. The characterization of *nif* gene products besides the nitrogenase components NifH, NifD, and NifK of *Azotobacter* identified NifS as a cysteine desulfurase that provides activated sulfur for cluster assembly in form of an enzyme-bound persulfide yielding L-alanine as the byproduct (3). A related protein is encoded outside the *nif* operon and has counterparts in non-nitrogen-fixing bacteria (4) and yeast (5, 6). It was termed IscS or NFS1. Whereas NFS1 of yeast is required for viability (6), *iscS*$^-$ mutants of *Escherichia coli* can grow in medium supplemented with thiamine and nicotinic acid (7, 8). However, poor activities of several 4Fe-4S proteins were observed in these strains (8), and their tRNA lacked thiouridine (7). Therefore, a variety of metabolic pathways, which require activated sulfur, depend on IscS, at least in *E. coli*. This organism also contains two further IscS/NifS-like proteins termed CsdB and CSD. They have been grouped in a separate class of NifS-like proteins based on sequence comparisons (9). CsdB has been implicated in selenocysteine metabolism and selenophosphate synthesis (10), because it prefers selenocysteine instead of cysteine, forming L-alanine and selenium (see Ref. 11 for detailed kinetic studies of the three NifS-like proteins of *E. coli*). Most recently CsdB was shown to contribute to an *isc*-independent minor pathway for the assembly of Fe/S clusters in *E. coli* (12).

The cystine lyase C-DES[1] is another, but unique, member of the family of NifS-like proteins. It was isolated from the cyanobacterium *Synechocystis* by its capacity to direct 2Fe-2S cluster assembly of ferredoxin *in vitro* (13). The cysteinyl residue, which is conserved in the active site of orthodox NifS-like proteins, is lacking. In variance to the NifS-type reaction pathway, C-DES was found to perform a usual β-elimination reaction with L-cystine instead of L-cysteine as substrate (Reaction 1) (14),

* This study was supported by grants from the Italian Ministry of Instruction, University and Research (Grant PRIN2001–2003 to A. M.). The costs of publication of this article were defrayed in part by the payment of page charges. This article must therefore be hereby marked "*advertisement*" in accordance with 18 U.S.C. Section 1734 solely to indicate this fact.

*The atomic coordinates and structure factors (code 1N2T, 1N31) have been deposited in the Protein Data Bank, Research Collaboratory for Structural Bioinformatics, Rutgers University, New Brunswick, NJ (http://www.rcsb.org/).*

§ Both authors contributed equally to this work.

¶ To whom correspondence may be addressed: Max-Planck-Institut für Biochemie, Abt. Strukturforschung, Am Klopferspitz 18a, Martinsried 82152, Germany. Tel.: 49-89-8578-2732; Fax: 49-89-8578-3516; E-mail: kaiser@biochem.mpg.de.

** Present address: Dept. of Biochemistry, University of Oxford, South Parks Road, Oxford OX1 3QU, United Kingdom.

¶¶ To whom correspondence may be addressed: Biochemiezentrum Heidelberg, Im Neuenheimer Feld 501, D-69120 Heidelberg, Germany. Tel.: 6221-548517; Fax: 6221-546613; E-mail: fb8@sun0.urz.uni-heidelberg.de.

[1] The abbreviations used are: C-DES, cystine CS-lyase; *E* , C-DES$^N$ , N-terminal modified C-DES; *E** , C-DES$^{K223A}$ , C-DES, Lys-223 → Ala mutant; *E*P, C-DES$^N$, complexed with products; *E**S, C-DES$^{K223A}$, complexed with substrate; Fe/S, iron-sulphur; (tm)NifS, (*Thermotoga maritima*) cysteindesulfurase; CsdB, *E. coli* selenocysteine deselenase; PLP, pyridoxal 5′-phosphate; MOPS, 3-(*N*-morpholino)propanesulfonic acid; Bicine, *N*,*N*-bis-(2-hydroxyethyl)glycine; r.m.s.d., root mean square deviation; PEG, polyethylene glycol.

$$\text{Cystine} + H_2O \rightarrow \text{cysteine persulfide} + \text{pyruvate} + NH_3$$

REACTION 1

By solving the three-dimensional structure of an N-terminal modified C-DES (C-DES$^N$), it could be demonstrated that the labile product cysteine persulfide firmly bound in a hydrophobic pocket in the active site of C-DES (15). In comparison to NifS that generates a protein-based cysteinyl persulfide, C-DES seems to use an alternative enzymatic strategy to produce activated sulfur for biosynthetic purposes.

In this report, the interaction of C-DES$^N$ with both the preferred substrate cystine and cysteine was studied in solution by time-resolved absorption spectroscopy and in the crystalline state by polarized absorption microspectrophotometry (16–19). Furthermore, a catalytically inactive mutant, in which the PLP-binding lysine 223 was replaced by alanine (C-DES$^{K223A}$), was characterized both at the functional and the structural level. Combining these results with previous structural data (15), a detailed reaction sequence for $\beta$-elimination can now be postulated. A structural comparison of C-DES with other members of the NifS-like protein family (NifS (20) and CsdB (21)) is presented. Specific structural features of NifS-like proteins and implications for Fe-S cluster synthesis are discussed.

## EXPERIMENTAL PROCEDURES

*Chemicals and Buffers*—Citric acid, L-cystine, L-cysteine, ammonium sulfate, potassium phosphate, polyethylene glycol 8000, MOPS, sodium dithionite, and barium chloride were of the best commercially available quality and were used without further purification.

*Strains and Expression Plasmids for C-DES$^N$ and C-DES$^{K223A}$ Production*—C-DES production from *Escherichia coli* PR745/pSA16 cells was described previously (13). The plasmid encoding the N-terminal variant of C-DES was a derivative of pSA16. Plasmid pSA16 was cut with *Sph*I and *Xba*I and treated with exonuclease III/S1 nuclease, so that about 150 bp were removed. Filling in the termini, religation and transformation created a series of *E. coli* PR745 strains that were checked for C-DES activity. The manipulated region of plasmids conferring overproduction was sequenced. The plasmid that was selected for further studies (pSA15) proved to contain a fusion between the genes coding for the $\alpha$-peptide of the $\beta$-galactosidase system and C-DES as follows: ATGACCATGATTACGCCAAGCTTGCACCAATTT, whereby the underlined nucleotides stem from pUC19. Overproduction relying on *E. coli* PR 745/pSA15 showed some tendency to fade especially during growth on a large scale. Therefore, the 1.9-kbp fragment obtained from complete *Afl*III and limited *Eco*RI digestion of pSA15 was ligated to the 9.1-kbp portion of vector pBT306.1, which was prepared by *Pst*I plus *Eco*RI digestion of pBT306.1 (gift from Dr. G. Schumacher; the *Afl*III- and *Pst*I-generated ends had been filled in by using Klenow enzyme or T4 polymerase, respectively). The resultant plasmid, pBT15, was used with *E. coli* MC4100 as host for large-scale production of C-DES$^N$ (growth conditions: aerated LB-medium, 37 °C). Cells were harvested by centrifugation about 3 h after reaching the stationary phase.

The K223A mutation was introduced as follows. A DNA fragment of 790 bp upstream of the *Eco*RI site contained in the *c-des* gene (14) was subcloned into pTZ18U and transformed into *E. coli* CJ236. Infection with M13KO7 gave the single-stranded, uracil-containing antisense DNA. The mutagenic strand was synthesized using the primer 5′-CACCGGCCATGCATGGTTTGC-3′, which served to replace the lysine codon AAA by the alanine codon GCA (changed nucleotides are underlined). The reaction mixture was used for transformation of *E. coli* XL1Blue MRF′, and the relevant sequence stretch of a selected plasmid was checked. From this plasmid, the 336-bp *Bsp*120I-*Eco*RI fragment was retrieved and used to replace the respective wild type fragment of pSA16. *E. coli* PR745 was used as a host for expression of C-DES$^{K223A}$ as described for wild type C-DES (14).

*C-DES$^N$ Purification*—An optimized protocol that retained the Q-Sepharose chromatography of the original procedure (13, 14) was developed to purify C-DES$^N$. The protocol is equally suited to purify wild type C-DES as well as C-DES variants. Purification of C-DES$^N$ is described here. Frozen *E. coli* MC4100/pBT15 cells (45g) were thawed and resuspended in 85 ml of 50 mM MOPS/NaOH, pH 8.0, containing 5 mM dithiothreitol and 0.5 mM phenylmethylsulfonyl fluoride, and disrupted by sonication. After centrifugation ($10^5 \times g$, 1 h), 6.4 ml of 10% Polymin G-35, adjusted to pH 7.7, was added to the extract (6.4 g of protein) with stirring, and the precipitate was removed by centrifugation ($2 \times 10^4 \times g$, 1 h). The protein solution (95 ml) was then heated to 60 °C in a glass flask with gentle shaking for 5 min. After cooling, 30 ml of 50 mM MOPS/NaOH, pH 7.6, were added and the precipitate was removed by centrifugation ($1.2 \times 10^4 \times g$, 20 min). The supernatant (115 ml) was concentrated to 50 ml by ultrafiltration using a PM10 membrane and applied to Q-Sepharose FF (20 cm$^2$ × 10 cm, 20 cm/h) equilibrated with 50 mM Tris-HCl, pH 7.4, containing 0.3 mM dithiothreitol and 20 $\mu$M EDTA. The protein concentration of the sample was 5 mg/ml. After washing with 200 ml of buffer, a linear gradient (2l) to 120 mM Tris-HCl, pH 7.4, containing 230 mM NaCl, 0.3 mM dithiothreitol, and 20 $\mu$M EDTA was applied. C-DES$^N$-containing fractions (480 mg of protein) were adjusted to 10 mg/ml protein in 50 mM MOPS/KOH, pH 7.3, 1.1 M ammonium sulfate, 5 mM EDTA, and 0.3 mM dithiothreitol and immediately applied to a Sepharose CL-4B column (20 cm$^2$ × 35 cm, 10 cm/h) equilibrated with the sample buffer. Isocratic elution gave homogenous C-DES$^N$ (about 230 mg), which appeared after elution with about 1.4 liter of buffer. The protein was precipitated by ammonium sulfate (addition of 0.15 g of solid/ml), dissolved in a minimal volume of 10 mM MOPS/NaOH, pH 7.6, and transferred into this buffer via Sephadex G-25 gel filtration, which yielded the final preparation.

*Crystallization of C-DES$^N$ and C-DES$^{K223A}$*—Crystals of both C-DES$^N$ and C-DES$^{K223A}$ were grown at 20 °C using the sitting drop vapor diffusion method. In the case of C-DES$^N$, 2.55 $\mu$l of a solution containing 10.3 mg/ml protein, 10 mM MOPS, pH 7.6, were mixed with 1.55 $\mu$l of various precipitant solutions obtained by diluting up to 1.2-fold a stock solution containing 100 mM potassium phosphate, 50 mM citric acid, 27% (w/v) PEG 8000, 100 mM ammonium sulfate, pH 6.5. Finally, 0.45 $\mu$l of a solution containing 100 mM barium chloride was added to the drop. The drops were equilibrated against 0.5 ml of the corresponding precipitant solution. Yellow plate-like crystals appeared within 3 days in all but the wells with the most diluted precipitant solution. Crystals belonged to space group $P2_12_12_1$ with cell constants a = 62.4 Å, b = 65.4 Å, and c = 170.1 Å, containing two monomers per asymmetric unit (15). The K223A mutant was crystallized following the same protocol using a 2-fold dilution of the precipitant stock and a 7.7 mg/ml protein solution.

*Co-crystallization of C-DES$^N$ and C-DES$^{K223A}$ with Cystine and Cysteine*—Both C-DES$^N$ and the K223A mutant were co-crystallized with cystine and cysteine. In the case of cysteine, crystals were obtained with the same procedure as described for the crystallization of the unliganded forms, adding 10 mM cysteine to the precipitant solution. The final pH of the solution was 6.1. In the case of cystine, which is poorly soluble in PEG solutions, a few solid grains were added to the crystallization drops.

*Spectrophotometric Measurements in Solution*—The spectral changes in the steady-state and pre-steady-state stage of reactions catalyzed by C-DES$^N$ were recorded in the presence of the preferred substrate L-cystine or the poor substrate (14) L-cysteine, in a solution containing ~0.5 mg/ml C-DES$^N$, 50 mM Bicine, pH 8.0, at 20 °C. Steady-state absorption spectra were collected with a CARY400 spectrophotometer. Rapid reaction studies were carried out with a temperature-controlled stopped-flow apparatus manufactured by Applied Photophysics. The instrumental dead time of this system was 1 ms. Time courses were fitted with the equation describing a biphasic process, $y = y_o + a(1 - e^{-bx}) + c(1 - e^{-dx})$, *where* $y_o$ is the value of absorbance at $t = 0$, $a$ and $c$ are the amplitude of the phases, and $b$ and $d$ are the corresponding rate constants.

*Single-crystal Polarized Absorption Microspectrophotometric Measurements*—Single crystals were resuspended at least six times in a solution containing 100 mM potassium phosphate, 50 mM citric acid, 27% (w/v) PEG 8000, 100 mM ammonium sulfate at pH 6.5 and either 10 mM cysteine or solid grains of cystine for crystals grown in the presence of cysteine or cystine, respectively. Crystals were loaded in a quartz flow cell, and the replacement of the suspending medium for the different experiments was carried out by flowing solutions through the cell (22). The cell was mounted on the stage of a Zeiss MPM03 microspectrophotometer, equipped with a ×10 ultrafluar objective and a thermostatic apparatus. Polarized absorption spectra were recorded in the range between 280 and 700 nm, with the electric vector of the linearly polarized light parallel to crystal edges. All the experiments were carried out at 15 °C.

*Data Collection and Processing*—Data from frozen single crystals were collected at the synchrotron Beamline BW6 (DESY Hamburg) with a MAR charge-coupled device detector. Oscillation images where integrated using DENZO and scaled with SCALEPACK of the HKL suite (23).

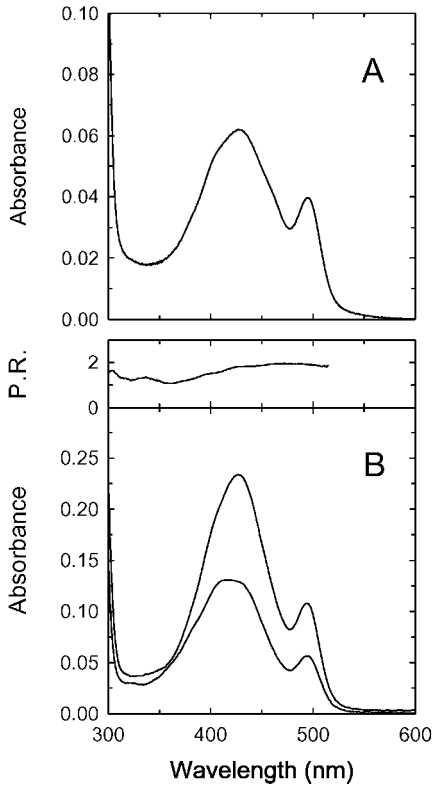


FIG. 1. **Absorption spectra of the internal aldimine of C-DES$^N$.** *A*, spectrum in a solution containing 0.5 mg/ml enzyme, 50 mM Bicine buffer, pH 8.0. *B*, polarized absorption spectra recorded on a single crystal of C-DES$^N$, suspended in a solution containing 27% PEG 8000, 50 mM citric acid, 100 mM potassium phosphate, 0.1 M ammonium sulfate at pH 6.5. Spectra were collected with light linearly polarized along crystal edges. *Upper panel*: polarization ratio.

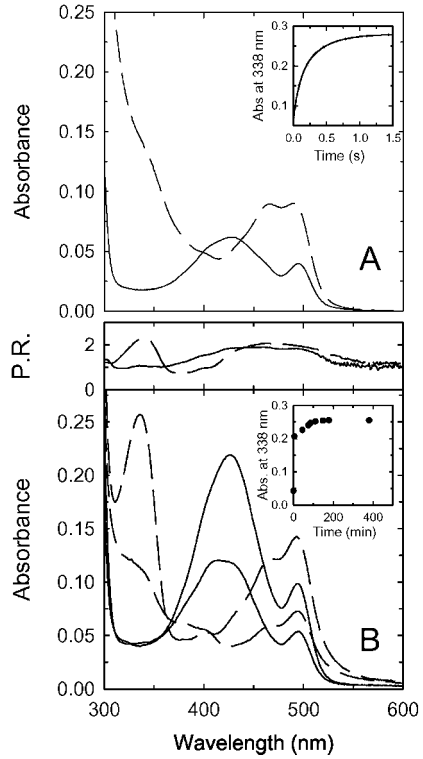


FIG. 2. **Reactivity of C-DES$^N$ with cystine in solution and in the crystal.** *A*, absorption spectra were recorded on a solution containing 0.5 mg/ml enzyme, 50 mM Bicine, pH 8.0, in the absence (*solid line*) and presence of 0.5 mM cystine (*dashed line*) after about 1 min of reaction time. *Inset*, time course of the reaction between 0.8 mg/ml enzyme and 5 mM cystine, 50 mM Bicine, pH 8.0. Only a limited number of data points are shown. The *solid line* through data points represents the fitting to a biexponential process (see "Experimental Procedures"). *B*, polarized absorption spectra of C-DES$^N$ crystals were recorded in a solution containing 27% PEG 8000, 50 mM citric acid, 100 mM potassium phosphate, 0.1 M ammonium sulfate, pH 6.5, in the absence (*solid line*) and presence of a saturated solution of cystine (*dashed lines*) after 4 h of reaction. *Upper panel*: polarization ratios of the spectra collected in the absence (*solid line*) and presence (*dashed line*) of cystine. *Inset*: time course of the reaction, monitored at 338 nm along the direction of polarization with more intense absorbance.

*Structure Solution and Refinement*—Molecular replacement was performed with MOLREP (24) using a polyalanine model of 1ELQ. Visual inspection of the electron density with partial rebuilding was performed with MAIN (25). Positional refinement, restrained *B*-factor refinement, and simulated annealing were performed with CNS (26) followed by additional rounds of side-chain rebuilding. Subsequently, a new water model was built. After visual inspection and manual water deleting, another round of simulated annealing was performed before the cofactor, and covalently linked groups were built. After a final cycle of water picking, deleting, refining of restrained individual *B*-factors, and positional refinement the models had final values of $R_{cryst}$ = 20.1, $R_{free}$ = 24.5 (*E**) and $R_{cryst}$ = 19.5, $R_{free}$ = 25.7 (*E**S), respectively. The structures have been deposited with the Protein Database, accession codes 1N2T and 1N31, respectively.

*Analysis and Graphical Representation*—Stereochemical parameters were assessed with PROCHECK (27). Protein structures were three-dimensionally aligned with TOP3D (24), and superimpositions were further refined with MAIN (25). The graphics in the figures were prepared with MOLSCRIPT, BOBSCRIPT (28, 29), and RASTER3D (30).

## RESULTS

*Absorption Spectra of C-DES$^N$*—A solution of native C-DES$^N$ was bright yellow, and its absorption spectrum was dominated by a band centered around 427 nm (Fig. 1*A*), corresponding to the protonated internal aldimine species formed between PLP and Lys-223. The intensity of the band did not change in the pH range between 6 and 11, indicating a p$K_a$ of the internal aldimine higher than 11. The observed ratio $A_{280\ nm}/A_{427\ nm}$ was 10. Spectra of C-DES$^N$ also showed a shoulder at 400 nm and a minor absorption band at 495 nm.

Polarized absorption spectra of the internal aldimine of C-DES$^N$ crystals exhibited two peaks at 427 and 495 nm (Fig. 1*B*), as in solution. The spectrum of lower intensity showed a broad peak centered at 420 nm, suggesting the presence of two or more overlapping bands. Crystals of the internal aldimine did not exhibit any spectral change in the pH range 6.0–8.0 (data not shown) and began to dissolve above pH 8.0, preventing experiments at higher pH values. The polarization ratio, *i.e.* the ratio of absorbance intensity at each wavelength, exhibited a value of about two both for the 427- and 495-nm peaks (Fig. 1*B*, *top panel*), suggesting a common orientation of the PLP ring and transition dipole moments for the two species.

*Absorption Spectra of C-DES$^N$ in the Presence of L-cystine*—To characterize the reaction catalyzed by C-DES, steady-state absorption spectra and stopped-flow spectroscopic studies were recorded at pH 8.0, upon mixing the enzyme with its preferred substrate L-cystine. The spectra (Fig. 2*A*) showed a decrease of the absorbance intensity at 427 nm and a concomitant appearance of a new absorbing species in the range of 310–380 nm. The exact $\lambda_{max}$ can be determined to be 338 nm based on the crystal spectrum (Fig. 2*B*) and is attributed to the external aldimine. Another species, absorbing at 470 nm, is interpreted as the PLP-aminoacrylate species. The intensity at 338 nm exhibited a fast biphasic increase with rate constants of 11 and 2.9 $s^{-1}$ and almost equal amplitudes, 0.42 and 0.58, respectively (Fig. 2, *inset*).

When crystals of C-DES$^N$ were suspended in a solution saturated with cystine, the polarized absorption spectra exhibited the appearance of an intense band at 337 nm and a weaker

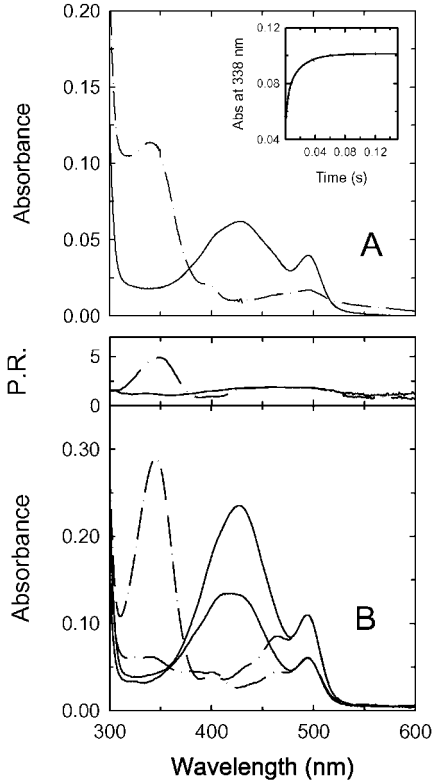


FIG. 3. **Reactivity of C-DES$^N$ with cysteine in solution and in the crystal.** *A*, absorption spectra were recorded on a solution containing 0.5 mg/ml enzyme, 50 mM Bicine, pH 8.0, in the absence (*solid line*) and presence of 10 mM cysteine (*dashed-dotted-dashed line*) after 1 min of reaction time. *Inset*, time course of the reaction between 0.8 mg/ml enzyme and 5 mM cysteine, 50 mM Bicine, pH 8.0. Only a limited number of data points are shown. The *solid line* through data points represents the fitting to a biexponential process (see "Experimental Procedures"). *B*, polarized absorption spectra of C-DES$^N$ crystals in a solution containing 27% PEG 8000, 50 mM citric acid, 100 mM potassium phosphate, 0.1 M ammonium sulfate, pH 6.5, in the absence (*solid line*) and presence of 10 mM cysteine (*dashed-dotted-dashed line*) after 30 min of reaction time. *Upper panel*: polarization ratios of spectra collected in the absence (*solid line*) and presence (*dashed-dotted-dashed line*) of cysteine.

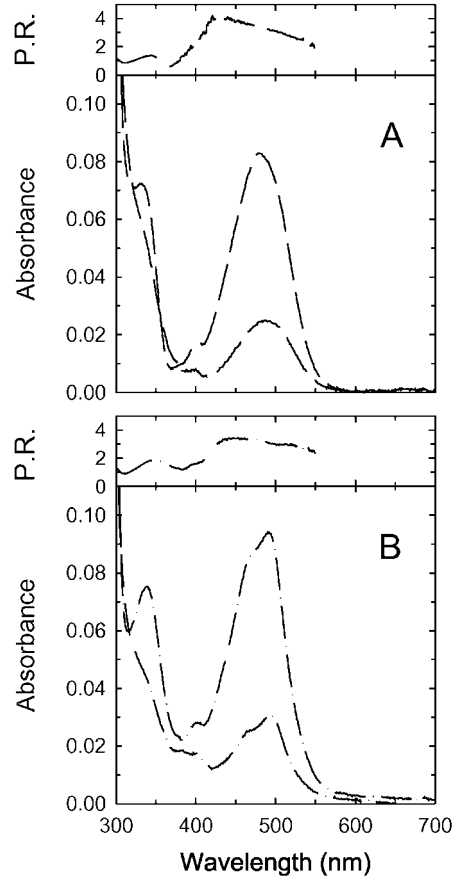


FIG. 4. **Polarized absorption spectra of C-DES$^N$ crystals, grown in the presence of cystine (*A*) and cysteine (*B*).** Crystals were suspended in a solution containing 27% PEG 8000, 50 mM citric acid, 100 mM potassium phosphate, 0.1 M ammonium sulfate, pH 6.4, and a saturating concentration of cystine and 10 mM cysteine, respectively. *Upper panels*: polarization ratio.

band at 470 nm, with the concomitant disappearance of the internal aldimine (Fig. 2*B*). The intensity of these bands slowly changed as a function of time (Fig. 2*B*, *inset*). The polarization ratio at 337 and 470 nm was about two (Fig. 2*B*, *top panel*).

*Absorption Spectra of C-DES$^N$ in the Presence of L-cysteine*—Steady-state spectra were recorded in the presence of L-cysteine (Fig. 3*A*), which is very slowly processed by C-DES to sulfide, pyruvate, and ammonia (14). Although the reaction mechanism of cysteine and cystine cleavage should be identical, the corresponding steady-state spectra exhibited striking differences. In the presence of cysteine, the absorption bands at 427 and 495 nm decreased with the concomitant formation of an intense band at 345 nm. The time course of the spectral changes at 345 nm was biphasic (Fig. 3*A*, *inset*) with rate constants of 308 and 53 $s^{-1}$ and equal amplitudes. The band at 470 nm, attributed to the α-aminoacrylate, was not observed under any experimental conditions, whereas a low intensity band at 400 nm was present.

Crystals of C-DES$^N$ in the presence of cysteine showed the disappearance of the peak at 427 nm and the appearance of bands at 345 and 470 nm (Fig. 3*B*). A low intensity peak at 400 nm indicated the presence of a poorly populated species, as in solution. These spectral changes occurred within the time of the replacement of solutions, ~5 min. However, on longer time scales (hours) the absorbance intensity decreased, likely due to a slow release of the external aldimine. Removal of cysteine, after a short incubation, led to a partial recovery of the original spectrum (data not shown). The band at 345 nm exhibited a polarization ratio of about five (Fig. 3*B*, *top panel*).

*Polarized Absorption Spectra of C-DES$^N$ Co-crystallized in the Presence of Either L-cystine or L-cysteine*—C-DES$^N$ crystals, grown in a precipitant solution saturated with cystine, exhibited a band at 480 nm that did not change even after removal of cystine and prolonged incubation in a cystine-free medium (Fig. 4*A*). Addition of sodium azide, a potential nucleophilic agent, previously shown to react with the α-aminoacrylate of *O*-acetylserinesulfhydrylase (18), did not affect the spectral properties. The band at 480 nm was similar in position to the marked shoulder observed either in C-DES$^N$ crystals grown in a solution containing 10 mM cysteine (Fig. 4*B*) or C-DES$^N$ crystals upon prolonged incubation with cysteine (data not shown). The polarized absorption spectra did not change significantly after removal of cysteine. The polarization ratio at 480 nm for both co-crystallized substrate-enzyme complexes was about four (Fig. 4, *top panels*).

*Absorption Spectra of C-DES$^{K223A}$ in the Presence and Absence of Cystine or Cysteine in Solution and in the Crystal*—The absorption spectrum of purified K223A mutant enzyme in solution exhibited a peak at 428 nm (Fig. 5*A*). Due to the replacement of the PLP-binding lysine by alanine, the coenzyme was not expected to form an internal aldimine species. However, the absorption spectrum was indicative of the formation of a Schiff base with another amino group, because the free coenzyme absorbs at 388 nm (31). Only subtle changes in the spectra were

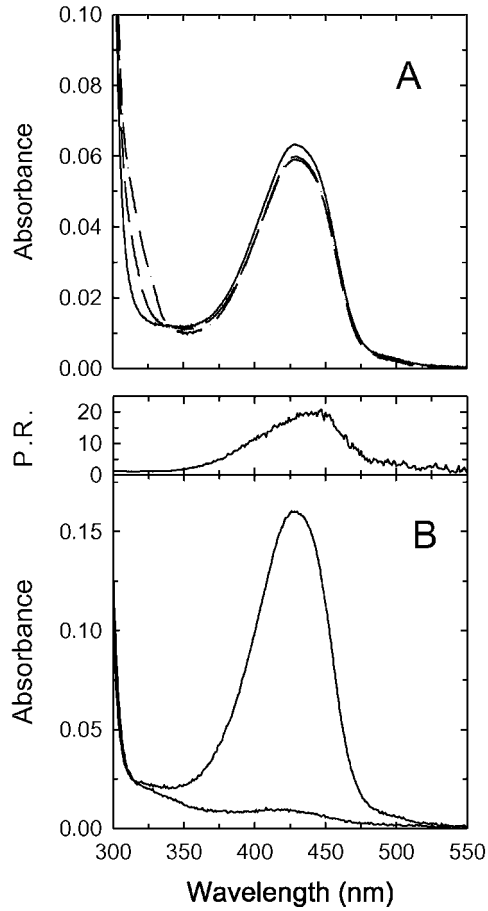


FIG. 5. **Absorption spectra of C-DES$^{K223A}$.** *A*, absorption spectra were recorded in a solution containing 0.5 mg/ml mutant enzyme, 50 mM Bicine, pH 8.0, in the absence (*solid line*) and presence of 0.5 mM cystine (*dashed line*) or 5 mM cysteine (*dashed-dotted-dashed line*). *B*, polarized absorption spectra collected on a single crystal of C-DES$^{K223A}$ suspended in a solution containing 27% PEG 8000, 50 mM citric acid, 100 mM potassium phosphate, 0.1 M ammonium sulfate, pH 6.5. *Upper panel*: polarization ratio.

observed when either L-cystine or L-cysteine was added to the reaction mixture (Fig. 5*A*).

Polarized absorption spectra of crystals of the K223A mutant showed a single peak at 426 nm (Fig. 5*B*), characterized by a high polarization ratio (Fig. 5*B*, *top panel*), indicating a well-defined orientation of the coenzyme within the active site. As in solution, the spectrum was only slightly affected by the presence of either cysteine or cystine (data not shown).

*Crystal Structure of the Michaelis Complex*—The structures of C-DES$^{K223A}$ (*E**) and of the C-DES$^{K223A}$/cystine (*E**S) complex were solved by molecular replacement. The *E** form was refined at 2.0 Å to a final crystallographic *R* value of 20.1 ($R_{free}$ = 24.5), the *E**S complex at 2.2 Å to a final $R_{cryst}$ of 19.5 ($R_{free}$ = 25.7). Both models show good stereochemical quality with over 91% of the residues in the favored regions of the Ramachandran diagram. Data collection and refinement statistics are summarized in Tables I and II, respectively.

In the active sites of both *E** and *E**S, the electron density for the PLP cofactor, which was omitted from the density calculation, was clearly visible (Fig. 6, *A* and *B*). In addition, in both forms additional electron density extended from C4A toward Arg-369. In the *E** form this electron density was modeled as an external aldimine with a captured glycine.

In *E**S the positive difference electron density accounts for the substrate cystine, which was covalently linked to the PLP, thus representing the external aldimine of the reaction. This

TABLE I
*Data collection statistics*

| | *E** | *E**S[a] |
|---|---|---|
| Wavelength, Å | 1.05 | 1.05 |
| Resolution, Å | 2.0 | 2.2 |
| Completeness, % | 96.5 | 95.3 |
| $R_{sym}$, % | 7.4 | 6.2 |

[a] *E**, Lys-223 → Ala mutant of C-DES; *E**S, Lys-223 → Ala mutant with substrate (cystine).

TABLE II
*Refinement statistics*

| | *E** | *E**S[a] |
|---|---|---|
| $R_{cryst}$ ($R_{free}$), % | 20.1 (24.5) | 19.5 (25.7) |
| Independent reflections | 47,830 | 35,389 |
| r.m.s.d. bonds, Å | 0.001 | 0.009 |
| r.m.s.d. angles, ° | 1.37 | 1.38 |
| r.m.s.d. bonded *B*-factors, Å$^2$ | 2.5 | 2.0 |
| Ramachandran plot | | |
| Favoured | 91.3 | 92.6 |
| Allowed | 8.4 | 8.6 |
| Additionally allowed | 0.3 | 0.2 |
| Number of atoms | | |
| Protein and ligand | 6,050 | 6,042 |
| Water | 593 | 734 |
| Ions | 2 | 2 |

[a] *E**, Lys-223 → Ala mutant; *E**S, Lys-223 → Ala mutant with substrate.

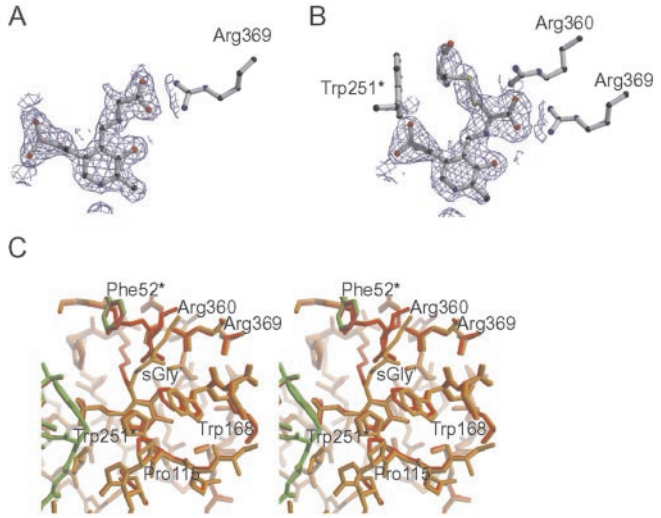


FIG. 6. **Electron density ($2F_o - F_c$) around the cofactor of C-DES$^{K223A}$ (*E**) and C-DES$^{K223A}$/cystine (*E**S).** *A*, in *E** the electron density can be interpreted in terms of an external aldimine between PLP and glycine. *B*, in the *E**S structure the extended conformation in subunit B is shown. The two arginines 360 and 369 that anchor the carboxylate groups and Trp-251 from the neighboring subunit are also shown. *C*, superposition of C-DES$^{N}$ structure (*E*) (subunit A, *red*; subunit B, *magenta*) and *E** (subunit A, *yellow*; subunit B, *light green*). Differences arise in positions of residues Trp-168 and Pro115 mediated through the binding of the "substrate" glycine to Arg-369. The positions of atoms of Trp-251* are unchanged between the structures.

extra electron density protruding from the cofactor differed between the two subunits in the crystallographic asymmetric unit. In subunit B it was interpreted as cystine in extended conformation being spanned between Arg-369 and Trp-251* (Fig. 6*B*). The electron density in subunit A was interpreted as a cystine in bent conformation, bound with its two carboxylate groups to Arg-360 and Arg-369, respectively, although the low quality of the density in this subunit suggests that several conformations are present in the crystal. Due to the limitation in resolution and the quality of the electron density, no other conformations where built. The flexibility of the substrate in

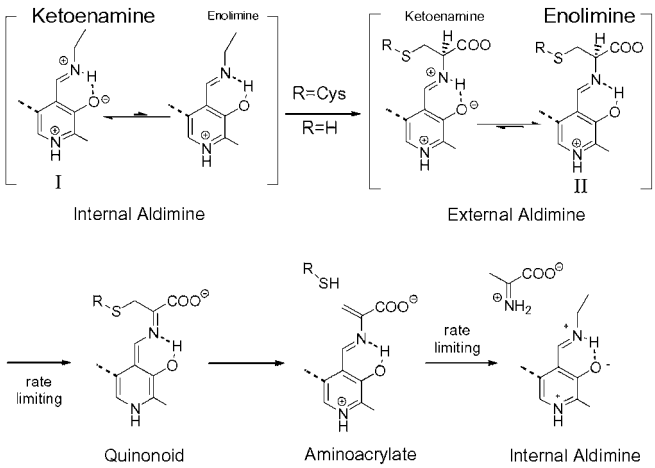


SCHEME 1

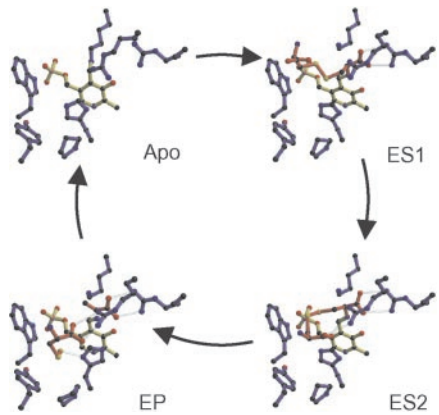


FIG. 7. **Crystallographically determined reaction cycle of C-DES.** Crucial residues are depicted as *blue sticks*; the cofactor is in *yellow sticks* with the substrate attached. Atoms are colored as follows: carbon, *black*; oxygen, *red*; nitrogen, *blue*; and phosphorus, *violet*.

the active site is also reflected by the rather high temperature factors as compared with the surrounding protein. A detailed description of side-chain movements between the native, *E**S, and product complexed (*E*P) forms is presented under "Discussion."

The benefit of *E** as a model for active C-DES can be inferred from the comparison of the unliganded C-DES$^{N}$ structure (1ELQ) with the unliganded C-DES$^{K223A}$ model, which show an r.m.s.d. of 0.1 Å over all $C_\alpha$ atoms (Fig. 6*C*). Except for Trp-168 (which moves by about 0.5 Å) and Pro-115 (which rotates about 8°) no side-chain movements were observed in the active site between the two structures. These small readjustments were necessary to accommodate for the carboxylate group of the PLP-bound glycine, which is salt-bridged to Arg-369, thereby displacing Trp-168 and, concomitantly, Pro-115.

*Comparison of C-DES, CsdB, and tmNifS*—As expected from the sequence homology, all three structures show a high degree of similarity concerning the overall fold. C-DES was aligned to tmNifS with an r.m.s.d. of 1.1 Å for 153 $C_a$ atoms, to CsdB with a deviation of 1.0 Å for 175 $C_\alpha$ atoms. A description of differences and similarities among the three structures is given under "Discussion."

## DISCUSSION

The net reaction of C-DES consists of the elimination of the $C_\beta$ substituent of L-cystine and various cystine analogues. The different covalent intermediates formed during PLP-dependent catalysis exhibit characteristic UV-visible spectra. Thus, the analyses of spectral changes that accompany substrate turnover contribute substantially to the mechanistic understanding of this enzyme implicated in Fe/S-cluster biosynthesis.

In analogy to other well characterized $\beta$-lyases, the reaction with cystine is associated with a fast disappearance of the internal aldimine, absorbing at 427 nm, and the concomitant formation of a species absorbing at about 340 nm, and a band at 470 nm, attributed to the ketoenamine tautomer of the aminoacrylate. The enolimine tautomer of the $\alpha$-aminoacrylate usually absorbs at 340–350 nm, the enolimine tautomer of external aldimines at 330–340 nm, and the geminal diamine at 320–330 nm. Thus, all three intermediates are likely candidates for the 340-nm absorbing species, with the quite unstable and low absorbing geminal diamine being the most unlikely one. Most probably, both enolimine tautomers contribute to the 340-nm absorption. In any case, the results suggest a clear preference for an enolimine form. Pursuant to this, the C-DES-catalyzed conversion of cystine should proceed as indicated in Scheme 1. Most remarkably, the tautomerization equilibrium of the protonated aldimines is inverted in the enzyme-substrate complex with respect to the internal aldimine. The ketoenamine is the predominant tautomer in the absence of substrate, whereas the neutral enolimine dominates upon substrate binding. Because this tautomer prefers a non-polar environment (32), the change in the tautomer equilibrium indicates an increased hydrophobicity of the environment around the aldimine linkage, which is essential for subsequent product stabilization.

Steady-state spectra recorded in the presence of cystine or cysteine reflect the rate-determining steps of the individual reactions. Interestingly, the spectra collected in the presence of the two closely related compounds suggest different key intermediates and thus distinct rate-limiting steps. For cysteine turnover, $\alpha$-proton abstraction from the external aldimine is rate-limiting, whereas conversion of the aminoacrylate-enzyme intermediate is the critical step during cystine turnover. As indicated in Scheme 1, these results can be rationalized in the light of the recently solved crystal structure of C-DES complexed with its reaction products (15). One key observation derived from the experiments in the crystalline state is the formation of a species absorbing at 470–480 nm after either prolonged incubation or co-crystallization with cystine or cysteine. Under the crystallization conditions used, this species is the predominant reaction intermediate and, on the basis of x-ray crystallographic data, has been identified as the $\alpha$-aminoacrylate (15). In contrast to aminoacrylate species formed by other PLP-dependent enzymes catalyzing $\beta$-elimination and $\beta$-replacement reactions (33, 34), the C-DES aminoacrylate is remarkably stable under crystallization conditions. This is partially due to the low pH of 6.5, where C-DES only displays 8% of its maximal activity, which is observed at pH 8.5; presumably this property reflects a particularly "locked" state of the active site, which impedes reverse transaldimination and concomitant release of iminopropionate. Cysteine persulfide, the product of cystine cleavage, is bound in the active site forming several, specific interactions. It is anchored on the solvent-accessible side of the PLP system, thereby capturing the aminoacrylate-enzyme intermediate and preventing further proceedings in the reaction. Obviously, the scissile "side chain" of cysteine, $H_2S$, is too small to fulfill a similar locking function. In solution this "locking" is somewhat weakened, and cysteine persulfide leaves the active site, which allows a coupled indicator reaction to be used to detect pyruvate as the final product of the C-DES reaction. Nevertheless, our results provide direct spectroscopic evidence that C-DES stabilizes its reaction products. To which extent this stabilization is maintained in solution remains to be proven. The polarization ratio of the 470- to

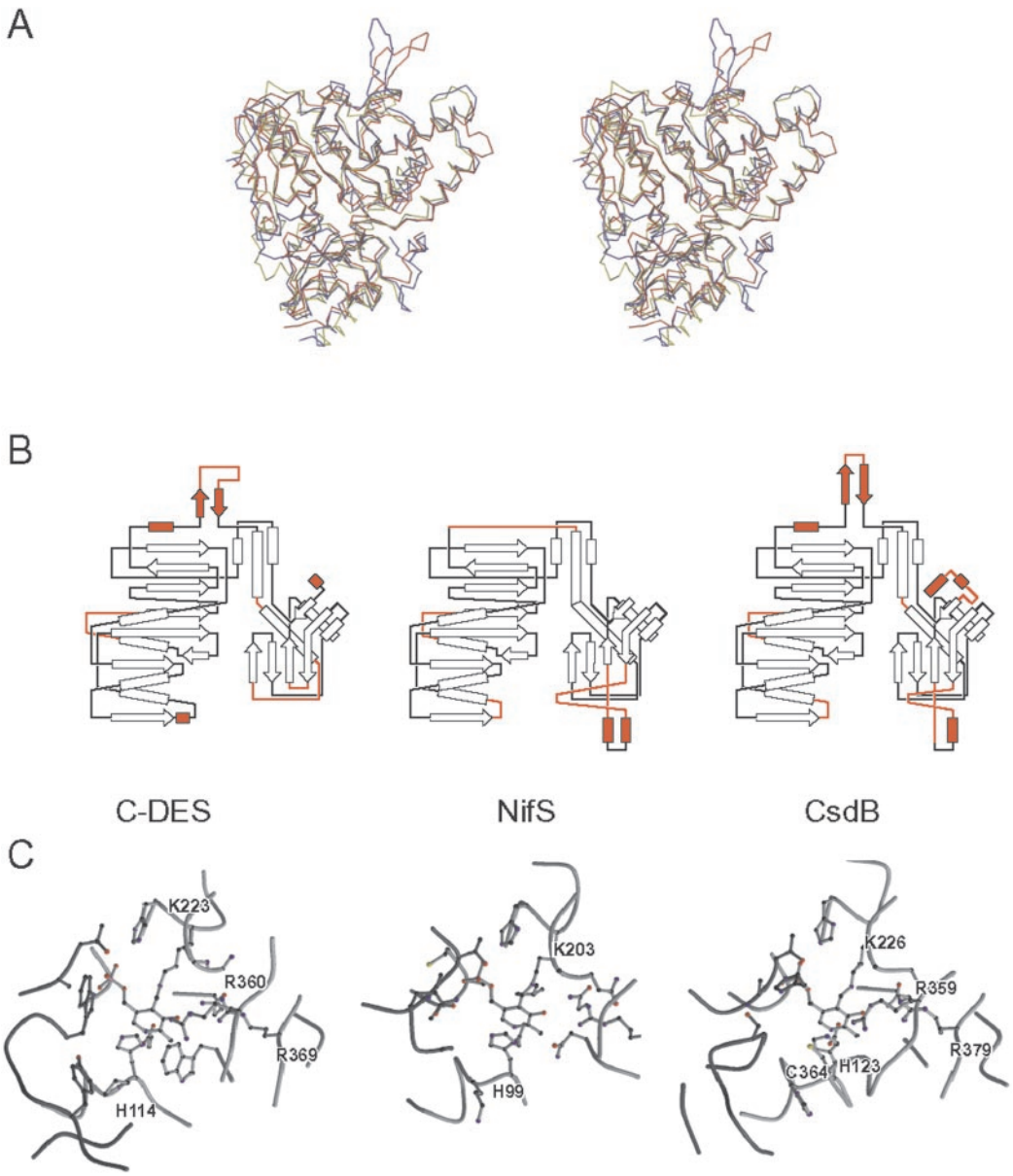


FIG. 8. **Comparison of C-DES, NifS, and CsdB.** *A*, stereo representation of the overlaid $C_\alpha$ traces: NifS (*yellow*), C-DES (*red*), and CsdB (*blue*). *B*, topology diagrams of C-DES, NifS, and CsdB with differences emphasized in *red*. *C*, comparison of the active sites of the three enzymes with critical residues labeled

480-nm band is about four, significantly different from that observed for the species absorbing at 470 nm, obtained immediately upon reaction with cystine and cysteine, suggesting that additionally a slow conformational change might have taken place causing a PLP ring reorientation.

The experiments carried out on crystals of C-DES$^N$ provide further evidence of the mechanism of catalysis, thus linking function to structure. Formation of the aminoacrylate- and external aldimine-enzyme complexes in the crystalline state indicates that the enzyme is catalytically competent in the reaction with cystine and cysteine. However, in the case of cysteine, the steady-state accumulation of catalytic species appears to be different in the crystal with respect to solution. In fact, a species absorbing at 470 nm, possibly aminoacrylate, is present, whereas no such species was observed in solution. This finding might be due to alteration of the rate-determining step associated to diffusion of substrates and products in and out the crystal channels. It is difficult to exclude that the aminoacrylate intermediate accumulates due to a small amount of cystine formed in the cysteine solution.

As compared with cystine cleavage showing the formation of a band at 338 nm, the steady-state intermediate of cysteine cleavage in the crystal exhibits a band at 345 nm, characterized by a polarization ratio close to five, different from those observed for the enolimine tautomers of L-cystine external aldimine and $\alpha$-aminoacrylate. This finding suggests that the enolimine tautomer of the external aldimine of cysteine possesses either a coenzyme orientation different from the enolimine tautomer of cystine, or the transition dipole moments directions of the two enolimines are significantly different. Unfortunately, due to crystal morphology, it is not possible to collect spectra in the third direction, thus preventing to obtain further information.

As in solution, the K223A mutant exhibits a spectrum characteristic of a Schiff-base linkage. As shown in Fig. 6*A*, in agreement with the spectroscopic data, the electron density can be interpreted as an external aldimine with a glycine acquired from the surrounding medium and anchoring its carboxylate group to Arg-360. The only subtle changes in the spectra when the K223A mutant is incubated with cysteine or cystine can be

attributed to a slow transaldimination reaction from the external Gly-aldimine to the external substrate-aldimine. The absence of the absorption at 338 nm, which was attributed to an enolimine species, can be explained in the light of the active site structure of the mutant. The place available upon Lys-223 → Ala replacement is occupied by three water molecules. Therefore the surrounding of the Schiff-base linkage in the mutant is much more hydrophilic thus favoring the ketoenamine species regardless of the bound ligand.

Concerning the crystallographic results for the early and late steps of the reaction, it is possible to draw the following picture. We assume that the substrate cystine is pre-oriented by binding with one of its carboxylate groups to Arg-369. Initially cystine is spanned in an extended conformation (*E**S1) between Arg-369 and Trp-251*. In this binding mode, the distal substrate carboxylate group is 5.6 Å from the guanidino group of Arg-360. Transaldimination to the external aldimine can take place with a concomitant rearrangement of cystine and Arg-360, gathering the distal carboxylate group of the substrate. In this way, cystine reorients into a bent conformation similar to the subsequently formed product molecules (*E**S2). On one hand, this rearrangement causes stress in the substrate SS bond, on the other hand, this leads to subtle side-chain movements in the active site. Trp-168 moves by about 0.8 Å away from the active site center. This residue forms part of the proximal wall of the active site and is in contact to His-114, the residue stacking to the cofactor. While moving, Trp-168 frees space for His-114 allowing it to rotate by about 20° around the $C_\beta$-$C_\gamma$ bond. This rotation is necessary to accommodate for the movement of the external aldimine-PLP adduct. In turn, the hydrophobic loop around Tyr-282* moves about 1.6 Å backward, thereby increasing the total hydrophobic surface area of the active site and, at the same time, forming the distal wall of the hydrophobic pocket, which finally stabilizes the cysteine persulfide product. During $\beta$-lysis His-114 moves by 1.8 Å toward Trp-168, thereby forming the final hydrophobic pocket. Interestingly, the substrate binding is accompanied with an opening of the enzyme of about 3.5 Å. This breathing is only observed in the substrate complexed form and cannot be attributed to specific movements. It is best reflected by the r.m.s.d. of the *E* to *E**S over all $C_\alpha$ atoms of 1.4 Å compared with the deviations of *E* to *E** and *E* to *E*P of 0.2 and 0.1 Å, respectively.

Using the crystallographic results for the early (*E*, *E**S1, *E**S2) and late steps (*E*P) and the spectroscopic results for the intermediate steps, it is now possible to draw a mechanism for the enzymatic action of C-DES (Fig. 7). The substrate cystine is acquired by C-DES in an extended conformation being spanned between Arg-369 and Trp-251*, permitting transaldimination in a relaxed substrate state. Subsequent rearrangement of the distal substrate carboxylate group toward Arg-360 positions cystine in a conformation similar to the products, which seems to be necessary for C-S bond cleavage. Concomitant movement of the active site residues around Gly-260* enlarges the hydrophobic distal wall of the active site, which is essential for persulfide stabilization. The increased hydrophobic nature of the active site is also reflected by the preference for the enolimine tautomer of the external aldimine. Subsequent substrate $C_\alpha$ deprotonation and $\beta$-lysis position the product cysteine persulfide in the hydrophobic pocket generated by Trp-251*, Tyr-256*, Pro-115, and His-114 and retains the aminoacrylate of PLP. The fact that hydrolysis of the aminoacrylate intermediate is rate-limiting points to the locking of this complex in an unreactive state. Reverse transaldimination yielding iminopropionate can only occur after cysteine persulfide is released from the active site. This explains the unusual stability of the ternary complex between enzyme, PLP-aminoacrylate, and cysteine persulfide thus suggesting a role of C-DES as persulfide carrier protein.

*Comparison of C-DES, CsdB, and tmNifS*—According to sequence similarities, C-DES, NifS (20), and CsdB (21) are all classified as NifS-like enzymes. Although the production of activated atomic chalcogen species is common to these proteins, they show remarkably distinct reactivities. In contrast to NifS, CsdB shows preference for selenocysteine over cysteine. This reactivity is not inhibited by thiol-alkylating agents, thus demonstrating a deviation from the mechanism proposed for cysteine desulfuration by NifS, although possessing the conserved cysteine residue in the C-terminal part of the protein. Not surprisingly, these agents do not inhibit C-DES, in which the active site Cys is absent. C-DES is compensating for this residue by using cystine as substrate, thereby mimicking it by the substrate itself. The most obvious structural difference is the absence of a large loop with partial $\beta$-structure in NifS, which forms the distal wall of the active site in C-DES and CsdB (Fig. 8). This part bears residues crucial for persulfide stabilization in C-DES, suggesting a similar mechanism of product stabilization for CsdB. Nevertheless, in the region of the distal wall, the active site of C-DES is by far the most closed due to Trp-251*. In CsdB the corresponding wall is constructed by Ala-125, Gly-253*, and Gly-277* in tmNifS by Gly-228* and Gly-237*. The preference for hydrophobic residues in this segment is evident, though the binding of the substrate in this region can lock probably only C-DES. Another remarkable difference concerning NifS, on one hand, and CsdB and C-DES, on the other hand, is the "Cys-324" loop. In NifS, where Cys-324 is crucial for function, this loop is by far the longest, composed of mainly hydrophilic and small residues (STSSACTSKDER in tmNifS) and disordered in the crystal structure. C-DES shows only a small turn and CsdB exhibits a short loop, composed of large and hydrophobic residues (VRTGHHCAMPL). This further points to the close relationship of C-DES and CsdB, whose functions seem not to depend on this flexible loop. As it has been suggested for NifS, this loop may act as a sulfur-delivery arm (20). C-DES and CsdB seem to supply their reaction products directly from the active site.

Remarkably, CsdB has an analogue to Arg-360 of C-DES, namely Arg-359. Both residues superimpose well, suggesting that possibly CsdB can utilize cystine or probably selenocystine as substrate. In the light of the finding that, at least in case of the selenocysteine-lyase activity of CsdB Cys-364, the homologue to Cys-324 in NifS, is not necessary, this similarity needs further investigation.

In summary, the family of NifS-like enzymes, although sharing remarkable sequence homologies, seems to perform catalysis by quite distinct mechanisms. In this work we have shown by combining spectroscopic and crystallographic results a possible mode of stabilization of the reaction product of C-DES, an, albeit quite unique, NifS-like enzyme. Comparative spectroscopic, biochemical, and crystallographic studies of more proteins of this interesting family of enzymes will surely help to understand the evolutionary relationship of a clan of "cofactor chaperones" required to build up the probably most ancient cofactor, the iron-sulfur cluster.

*Acknowledgments*—D. K. thanks J. Knappe for constant support and I. Leibrecht for technical assistance.

REFERENCES

1. Beinert, H., Holm, R. H., and Münck, E. (1997) *Science* **277,** 653–659
2. Johnson, M. K. (1998) *Curr. Opin. Chem. Biol.* **2,** 173–181
3. Zheng, L., White, R. H., Cash, V. L., Jack, R. F., and Dean, D. R. (1993) *Proc. Natl. Acad. Sci. U. S. A.* **90,** 2754–2758
4. Zheng, L., Cash, V. L., Flint, D. H., and Dean, D. R. (1998) *J. Biol. Chem.* **273,** 13264–13272
5. Strain, J., Lorenz, C. R., Bode, J., Garland, S., Smolen, G. A., Tall, D. T., Vickery, L. E., and Culotta, V. C. (1998) *J. Biol. Chem.* **273,** 31138–31144

6. Kispal, G., Csere, P., Prohl, C., and Lill, R. (1999) *EMBO J.* **18,** 3981–3989
7. Lauhon, C. T., and Kambampati, R. (2000) *J. Biol. Chem.* **275,** 20096–20103
8. Schwartz, C. J., Djaman, O., Imlay, J. A., and Kiley, P. J. (2000) *Proc. Natl. Acad. Sci. U. S. A.* **97,** 9009–9014
9. Mihara, H., Kurihara, T., Yoshimura, T., Soda, K., and Esaki, N. (1997) *J. Biol. Chem.* **272,** 22417–22424
10. Lacourciere, G. M., Mihara, H., Kurihara, T., Esaki, N., and Stadtman, T. C. (2000) *J. Biol. chem.* **275,** 23769–23773
11. Mihara, H., Kurihara, T., Yoshimura, T., and Esaki, N. (2000) *J. Biochem.* **127,** 559–567
12. Takahashi, Y., and Tokumoto, U. (2002) *J. Mol. Biol.* **277,** 28380–28383
13. Leibrecht, I., and Kessler, D. (1997) *J. Biol. Chem.* **272,** 10442–10447
14. Lang, T., and Kessler, D. (1999) *J. Biol. Chem.* **274,** 189–195
15. Clausen, T., Kaiser, J. T., Steegborn, C., Huber, R., and Kessler, D. (2000) *Proc. Natl. Acad. Sci. U. S. A.* **97,** 3856–3861
16. Mozzarelli, A., and Rossi, G. L. (1996) *Annu. Rev. Biophys. Biomol. Struct.* **25,** 343–365
17. Mozzarelli, A., Peracchi, A., Rossi, G. L., Ahmed, S. A., and Miles, E. W. (1989) *J. Biol. Chem.* **264,** 15774–15780
18. Mozzarelli, A., Bettati, S., Pucci, A. M., Burkhard, P., and Cook, P. F. (1998) *J. Mol. Biol.* **283,** 135–146
19. Bruno, S., Schiaretti, F., Burkhard, P., Kraus, J. P., Janosik, M., and Mozzarelli, A. (2001) *J. Biol. Chem.* **276,** 16–19
20. Kaiser, J. T., Clausen, T., Bourenkow, G. P., Bartunik, H. D., Steinbacher, S., and Huber, R. (2000) *J. Mol. Biol.* **297,** 451–464
21. Fujii, T., Maeda, M., Mihara, H., Kurihara, T., Esaki, N., and Hata, Y. (2000) *Biochemistry* **39,** 1263–1273
22. Mozzarelli, A., Ottonello, S., Rossi, G. L., and Fasella, P. (1979) *Eur. J. Biochem.* **98,** 173–179
23. Ottwinowski, Z., and Minor, W. (1997) *Methods Enzymol.* **276,** 307–326
24. Collaborative Computational Project Number 4 (1994) *Acta Crystallogr. Sect. D Biol. Crystallogr.* **50,** 760–763
25. Turk, D. (1996) in *Proceedings from the 1996 Meeting of the International Union of Crystallography Macromolecular Computing School* (Bourne, P. E., Watenpaugh, K., ed), www.sdsc.edu/Xtal/IUCr/CC/School96
26. Brunger, A. T., Adams, P. D., Clore, G. M., DeLano, W. L., Gros, P., Grosse-Kunstleve, R. W., Jiang, J.-S., Kuszewski, J., Nilges, N., Pannu, N. S., Read, R. J., Rice, L. M., Simonson, T., and Warren, G. L. (1998) *Acta Crystallogr. Sect. D Biol. Crystallogr.* **54,** 905–921
27. Laskowski, R. A., McArthur, M. W., Moss, D. S., and Thornton, J. M. (1993) *J. Appl. Cryst.* **26,** 283–291
28. Esnouf, R. M. (1997) *J. Mol. Graph. Model* **15,** 132–134
29. Kraulis, P. J. (1991) *J. Appl. Crystallogr.* **24,** 946–950
30. Merritt, E. A., and Murphy, M. E. P. (1994) *Acta Crystallogr. Sect. D Biol. Crystallogr.* **50,** 869–873
31. Kallen, R. G., Korpela, T., Martell, A. E., Matsushima, Y., Metzler, C. M., Metzler, D. E., Morozov, Y. V., Ralston, I. M., Savin, S. A., Torchinsky, Y. M., and Ueno, H. (1985) in *Transaminases* (Christen, P., and Metzler, D. E., eds) pp. 37–105, Wiley, New York
32. Faeder, E. J., and Hammes, G. G. (1971) *Biochemistry* **10,** 1041–1045
33. Miles, E. W. (1979) *Adv. Enzymol. Relat. Areas Mol. Biol.* **49,** 127–186
34. Cook, P. F., Hara, S., Nalabolou, S., and Schnackerz, K. D. (1992) *Biochemistry* **31,** 2298–2303

# Snapshots of the Cystine Lyase C-DES during Catalysis: STUDIES IN SOLUTION AND IN THE CRYSTALLINE STATE

Jens T. Kaiser, Stefano Bruno, Tim Clausen, Robert Huber, Francesca Schiaretti, Andrea Mozzarelli and Dorothea Kessler

*J. Biol. Chem. 2003, 278:357-365.*
*doi: 10.1074/jbc.M209862200 originally published online October 16, 2002*

---